

**THE FEATURES OF MULTIYEAR CHANGES AND SEASONAL VARIABILITY OF PRESENT-DAY BACKGROUND CONCENTRATIONS OF CO<sub>2</sub>, CH<sub>4</sub>, AND N<sub>2</sub>O AT THE GLOBAL MONITORING STATIONS**

*S.M. Semenov<sup>1,2)</sup>, E.Ya. Ran'kova<sup>1,2)</sup>*

<sup>1)</sup>Yu. A. Izrael Institute of Global Climate and Ecology,  
20B, Glebovskaya str., 107258, Moscow, Russia; *SergeySemenov1@yandex.ru*

<sup>2)</sup>Institute of Geography of the Russian Academy of Sciences,  
29, Staromonetny lane, 119017, Moscow, Russia

**Abstract.** Monthly data on concentrations of carbon dioxide CO<sub>2</sub>, methane CH<sub>4</sub> and nitrous oxide N<sub>2</sub>O obtained from 11 stations of the CSIRO GASLAB Flask Sampling Network are used. The stations monitor background concentrations in the surface layer of the atmosphere. Multiyear changes are studied with the time series of 12-month running averages. Seasonal variability is examined using differences between the series of bimestrial running averages and 12-month running averages. Close similarity of long-term trends at different stations has been found for each gas. The time series of seasonal deviations from stations situated at different extratropical latitudes, after adjustment for respective seasonal shifts, also reveal strong correlation for CH<sub>4</sub> and CO<sub>2</sub>, but not for N<sub>2</sub>O. The results support the hypothesis that seasonal variations of solar radiation flux in the lower atmosphere is the leading factor of the seasonal variability of CH<sub>4</sub> and CO<sub>2</sub> concentrations. Seasonal increase in the flux causes the enhancement of CO<sub>2</sub> photosynthetic uptake by terrestrial and ocean plants. Simultaneously, the level of hydroxyl in the atmosphere increases that intensifies methane depletion in the troposphere.

**Keywords.** Carbon dioxide, methane, nitrous oxide, global monitoring stations, similarity, long-term changes, seasonal variations.

**ОСОБЕННОСТИ МНОГОЛЕТНИХ ИЗМЕНЕНИЙ И СЕЗОННОЙ ИЗМЕНЧИВОСТИ СОВРЕМЕННЫХ ФОНОВЫХ КОНЦЕНТРАЦИЙ СО<sub>2</sub>, СН<sub>4</sub> И N<sub>2</sub>O НА СТАНЦИЯХ ГЛОБАЛЬНОГО МОНИТОРИНГА**

*С.М. Семенов<sup>1,2)</sup>, Э.Я. Ранькова<sup>1,2)</sup>*

<sup>1)</sup> Институт глобального климата и экологии имени академика Ю.А. Израэля,  
Россия, 107258, Москва, ул. Глебовская, 20Б; *SergeySemenov1@yandex.ru*

<sup>2)</sup> Институт географии РАН,  
Россия, 119017, Москва, Старомонетный пер., 29

**Реферат.** Использованы месячные данные о содержании углекислого газа CO<sub>2</sub>, метана CH<sub>4</sub> и закиси азота N<sub>2</sub>O на 11 станциях сети CSIRO GASLAB

Flask Sampling Network. Это станции глобального мониторинга фоновых концентраций в приповерхностном слое атмосферы. Многолетние изменения изучались с помощью рядов 12-тимесячных скользящих средних значений. Сезонная изменчивость исследовалась по разности рядов двухмесячных и 12-тимесячных скользящих средних значений. Обнаружено высокое сходство многолетних трендов на разных станциях для каждого из газов. Ряды сезонных девиаций на станциях, расположенных на разных внетропических широтах, с учетом соответствующих сезонных сдвигов также обнаружили высокое корреляционное сходство для  $\text{CO}_2$  и  $\text{CH}_4$ , но не для  $\text{N}_2\text{O}$ . Результаты позволяют предположить, что ведущим фактором сезонной изменчивости  $\text{CO}_2$  и  $\text{CH}_4$  являются сезонные вариации потока солнечной радиации в нижней атмосфере. В сезон усиления потока и стимулируется поглощение  $\text{CO}_2$  наземными и океанскими растениями в ходе фотосинтеза, и увеличивается уровень содержания гидроксила в атмосфере, что ускоряет процесс разрушения метана в тропосфере.

**Ключевые слова.** Углекислый газ, метан, закись азота, станции глобального мониторинга, сходство, многолетние изменения, сезонные вариации.

## Introduction

Carbon dioxide  $\text{CO}_2$ , methane  $\text{CH}_4$ , and nitrous oxide  $\text{N}_2\text{O}$  are the major greenhouse gases emitted to the atmosphere due to anthropogenic activity. Enrichment of the atmosphere with these gases causes a worldwide concern regarding the growing greenhouse effect. In 2011, the gases' radiative forcing was the greatest and equal to, respectively,  $1.82 \pm 0.19$ ,  $0.48 \pm 0.05$  and  $0.17 \pm 0.03 \text{ W m}^{-2}$  (compared to the preindustrial period<sup>1</sup>). The total radiative forcing of all well-mixed greenhouse gases was 2.83 (from 2.54 to 3.12)  $\text{W m}^{-2}$  (Myhre et al., 2013, p. 676). Therefore, present-day changes in the global levels of those gases in the atmosphere are the subject for continuous monitoring and subsequent studies.

$\text{CO}_2$ ,  $\text{CH}_4$ , and  $\text{N}_2\text{O}$  are well-mixed gases, i.e., their lifetime in the atmosphere characterizing irreversible or reversible removal from the atmosphere substantially exceeds the characteristic time of their transmission and mixing in the troposphere both in horizontal and vertical directions. The outcome is the approximate equalizing of concentrations (expressed as VMR, volume mixing ratio) at different points of geographical space that are not directly influenced by particular substantial local or regional emission sources. Thus, the concentrations are close, but not equal, neither constant in time.

Long-term changes and seasonal variability of  $\text{CH}_4$  levels were considered in detail in our earlier publication (Semenov, 2018). In this paper, only new estimates of multiyear averages of seasonal deviations of methane concentration will be presented. In relation to the other two gases, namely  $\text{CO}_2$  and  $\text{N}_2\text{O}$ , the aim of this work is to study the following issues using monitoring data from the network of The Commonwealth Scientific and Industrial Research Organisation (CSIRO):

---

<sup>1</sup>) Preindustrial period: conventionally, before 1750.

---

- long-term and seasonal changes of global background concentrations of these gases in the surface layer of the atmosphere;
- similarity and differences of these variations at different latitudes of the Northern and Southern Hemispheres;
- features of those changes and their possible connections with factors governing the formation of levels of these gases.

### Data and methods

Data on global background concentrations of CO<sub>2</sub>, CH<sub>4</sub> and N<sub>2</sub>O from 11 sampling stations of CSIRO network (CSIRO GASLAB Flask Sampling Network, <http://cdiac.ess-dive.lbl.gov/trends/co2/csiro/>) were used. Locations of those stations are displayed in Fig. 1, their names are given in Table 1.

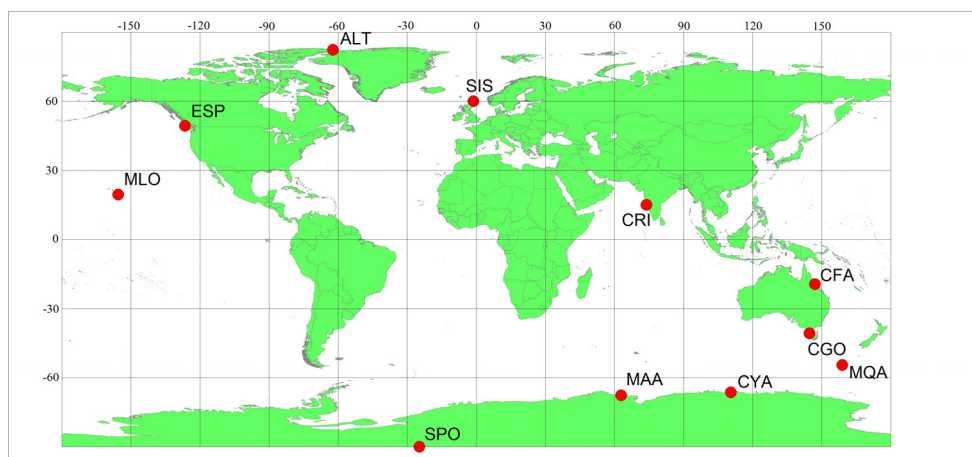


**Figure 1.** CSIRO GASLAB Flask Sampling Network (<http://cdiac.ess-dive.lbl.gov/trends/co2/csiro/>)

**Table 1.** Names and locations of CSIRO stations

Abbreviation	Name	Location
ALT	Alert	Canada
ESP	Estevan Point	Canada
SIS	Shetland Islands	UK
MLO	Mauna Loa	USA
CRI	Cape Rama	India
CFA	Cape Ferguson	Australia
CGO	Cape Grim	Australia
CYA	Casey	Antarctic
MAA	Mawson	Antarctic
MQA	Macquarie Island	Australia
SPO	South Pole	Antarctic

Measurements of CO<sub>2</sub>, CH<sub>4</sub>, and N<sub>2</sub>O concentrations were carried out at this sampling network over last decades. D.M. Etheridge, P.B. Krummel, R.L. Langenfelds, L.P. Steele and other CSIRO leading scientists took part in this work. This paper uses the time series of monthly mean concentrations from the archive <CSIRO\_gaslab\_data\_Jul2015.zip>. The archive was downloaded from [http://cdiac.ess-dive.lbl.gov/trends/co2/modern\\_co2.html](http://cdiac.ess-dive.lbl.gov/trends/co2/modern_co2.html) (→DATA, →CSIRO) in March, 2018.

Geographical locations of those stations and the methodology for time series analysis employed in this paper were described in more details in (Semenov, 2018). Therefore, here the methodology is given in brief only.

For each station, three series are derived from its initial series of monthly mean concentrations <sup>2</sup> (see Fig. 2). The series are labelled as *A*, *B* and *B-A*:

*A*) the series of yearly running averages, i.e., means for 12 sequential months; the value is associated with 00:00 on the 1<sup>st</sup> day of the 7<sup>th</sup> month (the moment between the 6<sup>th</sup> and 7<sup>th</sup> months);

*B*) the series of bimestrial running averages, i.e., means for the 6<sup>th</sup> and 7<sup>th</sup> months; the value is associated with the same moment;

*B-A*) the difference between series *B* and *A*.

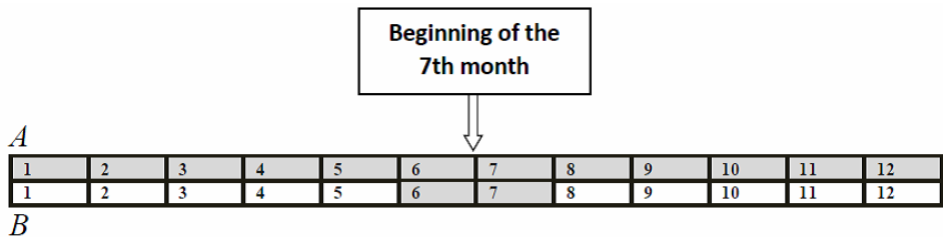


**Figure 2.** Construction of time series *A* and *B*. On two scales presenting the ‘running set’ of 12 sequential months, the time spans used for the construction of series *A* (the upper scale) and *B* (the lower scale) are shadowed; the results of averaging refer to the beginning of the 7<sup>th</sup> month

*A*-series are employed to describe changes in gases’ concentrations on the yearly time scale, i.e., using the 12-month running averages. (*B-A*)-series, i.e. series of seasonal deviations, are used to describe seasonal variability.

When comparing (*B-A*)-series from different points of geographical space and for different gases, different time shifts are applied. An ordered pair of series  $\{X(t)\}$  and  $\{Y(t)\}$  is always considered and a time shift is applied to the second series. This time shift means a transfer to the series  $\{Y(t + \tau)\}$ . If  $\tau > 0$ , the shift will be called a ‘backward shift for  $\tau$  months’, if  $\tau < 0$ , the shift will be called a ‘forward shift for  $|\tau|$  months’. The time shift  $\tau$ ,  $-6 \leq \tau \leq 6$ , yielding the maximal correlation is called ‘the optimal time shift’. The condition  $-6 \leq \tau \leq 6$  is applied, because addition or deduction of number of months multiple of 12 obviously does not change a season.

In this paper, (*B-A*)-series are also used in the estimation of multiyear intra-annual course of seasonal deviations of concentrations and their standard errors. It

---

<sup>2</sup>) Differences in duration of the months are ignored in these constructions.

should be noted that similarity of the course for a pair of series and similarity of multiyear series of seasonal deviations themselves are different concepts. The second concept infers the first one, but not *vice versa*.

## Results and discussion

### *Changes on the yearly time scale*

A-series for CO<sub>2</sub> and N<sub>2</sub>O for 11 stations are displayed in Figs. 3 and 4, respectively. In (Semenov, 2018), while analyzing such long-term changes in methane concentrations, we adjusted data to those from station Alert<sup>3</sup> through elimination of systematic deviations (bias). It was necessary, because annual mean concentrations of methane substantially differ at different latitudes, in different hemispheres. However, we did not do this for CO<sub>2</sub> and N<sub>2</sub>O, since after such adjustment the curves are practically coincided and are hardly distinguishable in the figures.

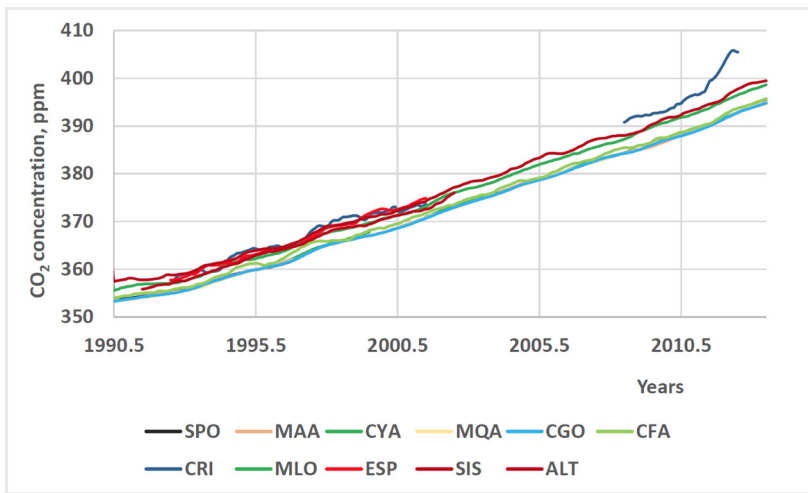


**Figure 3.** Long-term changes in CO<sub>2</sub> concentrations (ppm); 12-month running averages

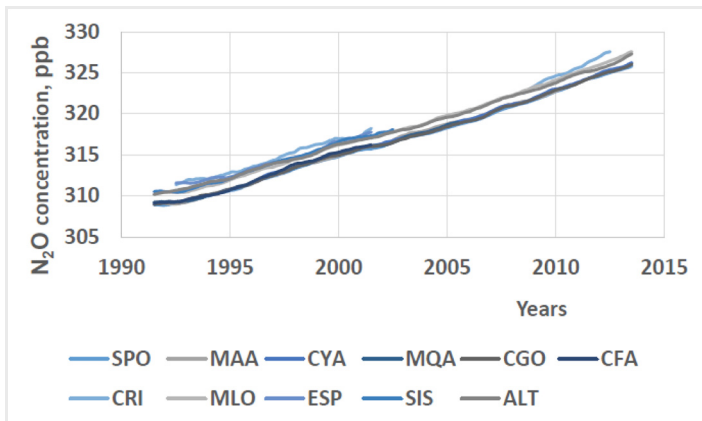


**Figure 4.** Long-term changes in N<sub>2</sub>O concentrations (ppb); 12-month running averages

<sup>3)</sup> The northernmost station of the Northern Hemisphere; its choice is conventional.

It is clear from Fig. 3 that different stations demonstrate similar CO<sub>2</sub> trends. The tropical station Cape Rama is an exception. Probably, it is substantially influenced by the regional sources of carbon dioxide.

Analogous data on nitrous oxide N<sub>2</sub>O are displayed in Fig. 4. Different stations demonstrate similar long-term trends of concentrations of this gas. This is also correct for station Cape Rama. In this case, the data from this station do not deviate substantially from others.

### *The intra-annual course of seasonal deviations of the gases' concentrations*

For each station and gas, the multiyear averages of elements of (*B-A*)-series associated with each of 12 calendar months<sup>4</sup> were calculated, and standard errors were also estimated. The intra-annual course of seasonal deviations obtained through this procedure will further be considered as seasonal course of concentrations. Results of the calculations for CO<sub>2</sub>, CH<sub>4</sub> and N<sub>2</sub>O are displayed in Figs. 5a, 5b, and 5c, respectively.

The solid curve indicates the inter-month variations of the multiyear averages. The vertical box boundaries show the  $\pm\sigma$  interval around the averages. The vertical span shows the full range of all values.

As seen in Fig. 5a, in both hemispheres the CO<sub>2</sub> level starts declining approximately at the beginning of the vegetative season, while the increase begins when the vegetative season ends up. This is completely in line with the concept on the role of plants (both terrestrial and oceanic) in photosynthetic CO<sub>2</sub> uptake from the atmosphere (Keeling et al., 2005). However, one should take into account, that in the warm season the effect of enhanced uptake due to increase in photosynthesis intensity could be partly offset by a decrease in CO<sub>2</sub> solubility in the surface ocean layer and an increase in physical release of CO<sub>2</sub> by the ocean.

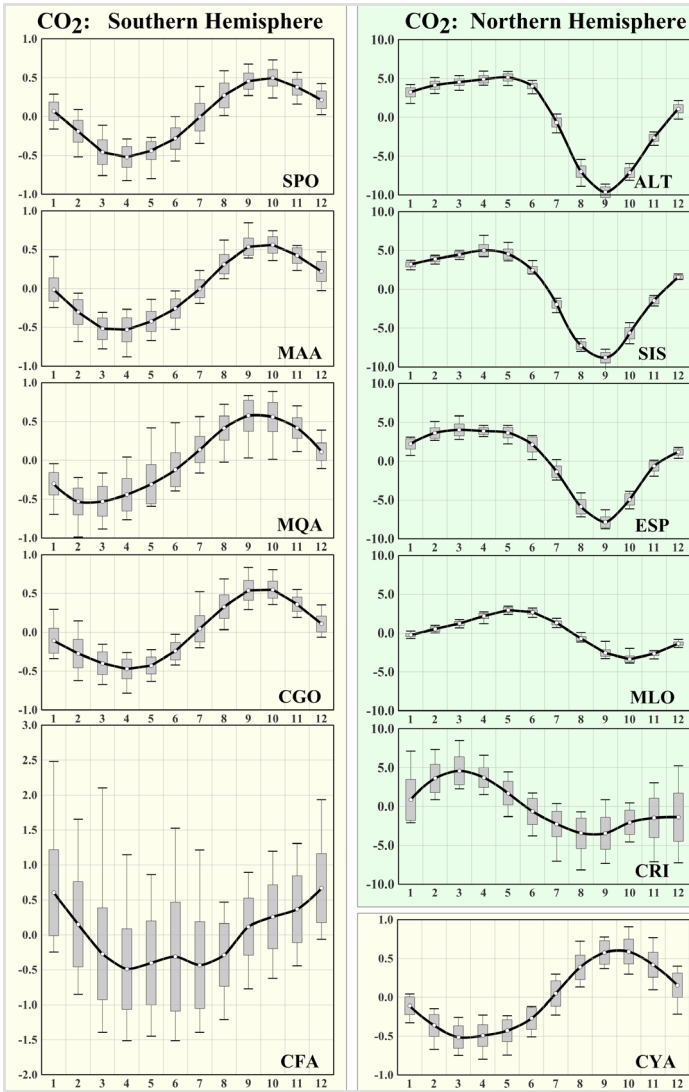
The seasonal variations at the tropical stations Cape Rama and Cape Ferguson are less pronounced, though mainly similar to those at the other stations. It is to note a peculiarity of the seasonal course at the Mauna Loa station situated at tropical latitudes: decrease of CO<sub>2</sub> level from the maximum begins somewhat later than at the more northern stations of the Northern Hemisphere. The same is correct for the beginning of increase in the level from the minimum. The issue requires special investigation. Perhaps, this can be explained with the high altitude location of the station (3 397 m above sea level). The other stations of the Northern Hemisphere are situated substantially lower. At the tropical station Cape Rama, decrease of the concentration from the maximum, as expected, begins earlier than at the extratropical stations of the Northern Hemisphere.

The periods of increase and decrease in the CO<sub>2</sub> level are very similar at all stations of the Southern Hemisphere.

---

<sup>4</sup> In Figs. 5a, 5b, and 5c, each of the multiyear averages (given at the vertical axis) relates to the second months (given at the horizontal axis) of the two respective sequential months from which the bimestrial running average value was calculated.

---



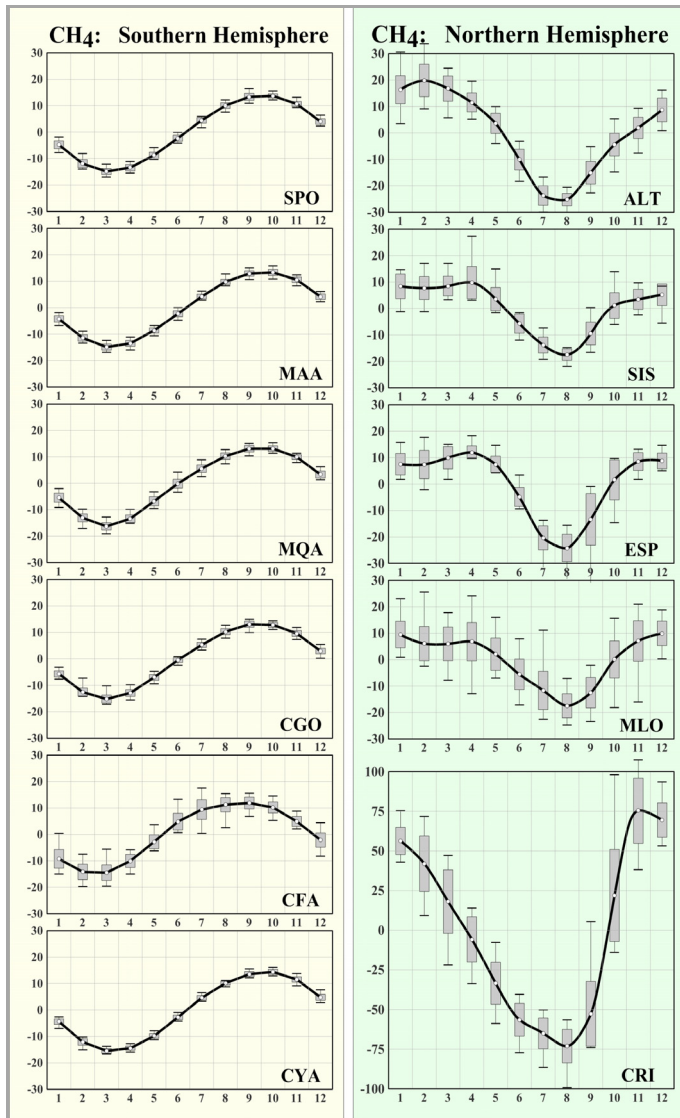
**Figure 5a.** Seasonal course of CO<sub>2</sub> concentration (ppm)

Figure 5b displays data on the seasonal course of CH<sub>4</sub> concentration. At all stations of the Southern Hemisphere periods of seasonal increase and decrease of the concentrations are very similar, as well as the form of yearly course curves. The level increases in spring to autumn<sup>5</sup> (the cold season), then the period of decrease is observed.

In the Northern Hemisphere, the curves' forms discernibly differ. However, almost at all stations pronounced decrease begins in spring and ends up by autumn (in August). Tropical station Cape Rama is an exception: there the increase period is much shorter and decrease resumes in November.

<sup>5)</sup> Hereinafter the seasons' names refer to the seasons of the Northern Hemisphere.

The seasonal course of CH<sub>4</sub> concentration presented in fig. 5b supports the following concept: the enrichment of the atmosphere with hydroxyl due to seasonal increase in the solar radiation flux reaching the Earth's surface plays a substantial role in the seasonal decline of methane level. The reaction with hydroxyl is the major sink of methane in the lower atmosphere (Voulgarakis et al., 2013).



**Figure 5b.** Seasonal course of CH<sub>4</sub> concentration (ppb)

Seasonal course of N<sub>2</sub>O concentration is presented in Fig. 5c. Variations are small, their amplitude is less than 0.5 ppb. Only at the tropical station Cape Rama it is somewhat greater. Inter-annual variability of seasonal deviations is also greater at this station, especially in the warm season. Seasonal course of nitrous oxide concentration is practically absent at the high altitude tropical station Mauna Loa (3 397 m above sea level).



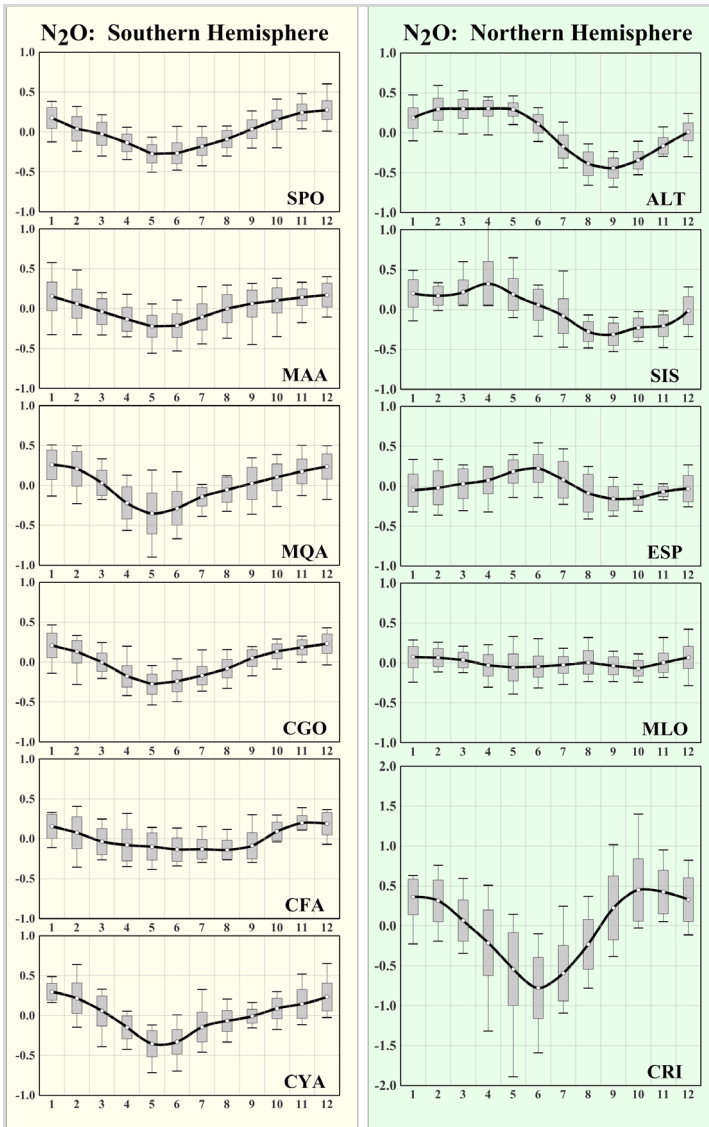


Figure 5c. Seasonal course of  $N_2O$  concentration (ppb)

### *Multiyear series of seasonal deviations*

Comparative analysis of seasonal deviations of  $CO_2$ ,  $CH_4$  and  $N_2O$  concentrations in the atmosphere at CSIRO network stations is performed as follows. For each ordered pair of stations the respective ( $B-A$ )-series are considered. The second station series is shifted in time relatively to the first one for several (from  $-6$  to  $6$ ) months. Then the correlation coefficient is calculated and the optimal shift ensuring its maximal value is found. Thus, rather than studying the similarity of the intra-annual course of seasonal deviations considered in the previous section, we study the similarity between the time series of seasonal deviations in this section.

Seasonal variations of CO<sub>2</sub>, CH<sub>4</sub> and N<sub>2</sub>O atmospheric concentrations at the global monitoring stations could be determined by three processes:

- air exchange in all directions between the ‘local part’ of the atmosphere and the global atmosphere (the global monitoring station location ensures the absence of influence of local sources);
- gas exchange with the ocean and land;
- depletion due to chemical reactions in the atmosphere.

These processes contribute differently to seasonal variations in the gases’ concentrations. The first process, atmospheric transmission, has both vertical and horizontal components and is common for all three gases. Its characteristic time does not exceed few months which is much lesser than the lifetime of the gases in the atmosphere that varies roughly from 10 to 100 years (Forster et al., 2007, section 2.10.2; Myhre et al., 2013). Can this process ensure the similarity of seasonal deviations of the gases’ concentrations at different stations?

Correlation coefficients for the series of N<sub>2</sub>O seasonal deviations are given in Table 3. In the majority of cases correlations ( $R$ ) are not high ( $R^2 < 0.5$ ), in particular, for the Northern Hemisphere stations. Noticeable similarity of the series of seasonal deviations at Alert (ALT), South Pole (SPO) and Cape Grim (CGO) stations ( $R^2 > 0.5$  under optimal time shifts) is an exception. While for SPO and CGO stations this can be explained by their relative geographical closeness, for the ALT and SPO pair as well as for the ALT and CGO pair this is not the case.

The time series for ALT and SPO stations are displayed in Fig. 6. Noticeable, although not high, similarity of the series requires further investigation.

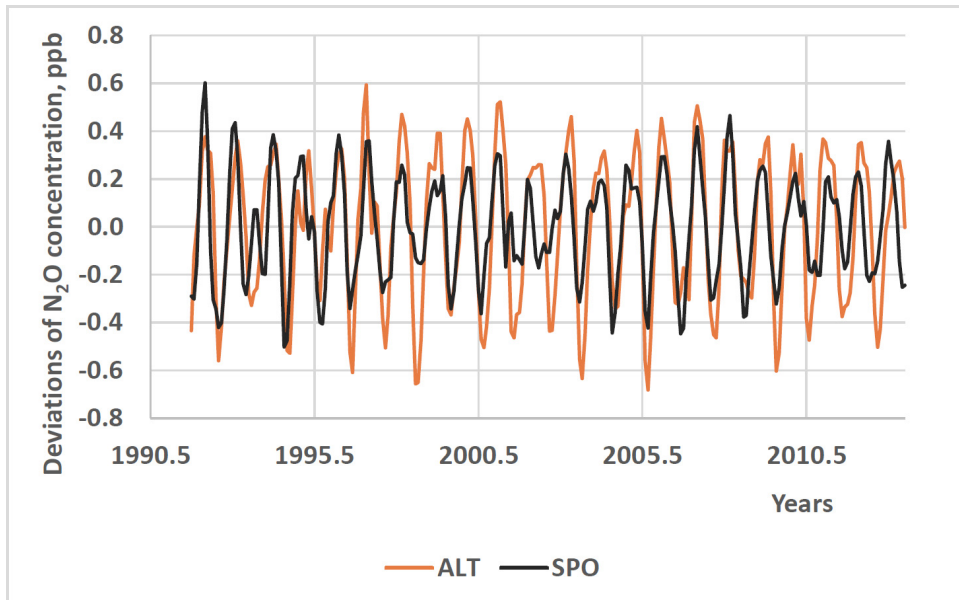


**Figure 6.** Seasonal deviations of N<sub>2</sub>O level at stations Alert (ALT) and South Pole (SPO), ppb; the series of the latter station is shifted forward in time for 3 months

**Table 3.** Estimates of correlations of the time series of seasonal deviations of N<sub>2</sub>O concentration\*

	SPO	MAA	CYA	MQA	CGO	CFA	CRI	MLO	ESP	SIS	ALT
SPO	1.00	0.56	0.67	0.54	0.80	0.53	0.62	0.32	0.34	0.50	0.72
	0	0	0	0	0	0	0	1	5	3	3
MAA	0.56	1.00	0.55	0.48	0.59	0.48	0.42	0.33	0.28	0.44	0.59
	0	0	0	0	0	0	1	1	5	4	4
CYA	0.67	0.55	1.00	0.65	0.67	0.54	0.58	0.30	0.67	0.48	0.67
	0	0	0	0	0	1	0	0	3	3	3
MQA	0.54	0.48	0.65	1.00	0.62	0.43	0.37	0.20	0.43	0.57	0.61
	0	0	0	0	0	0	0	-1	4	3	3
CGO	0.80	0.59	0.67	0.62	1.00	0.58	0.66	0.30	0.39	0.55	0.73
	0	0	0	0	0	1	0	1	5	3	3
CFA	0.53	0.48	0.54	0.43	0.58	1.00	0.39	0.34	0.38	0.41	0.56
	0	0	-1	0	-1	0	-1	2	6	2	3
CRI	0.62	0.42	0.58	0.37	0.66	0.39	1.00	0.29	0.28	0.64	0.71
	0	-1	0	0	0	1	0	3	-6	3	3
MLO	0.32	0.33	0.30	0.20	0.30	0.34	0.29	1.00	0.29	0.19	0.24
	-1	-1	0	1	-1	-2	-3	0	4	4	3
ESP	0.34	0.28	0.67	0.43	0.39	0.38	0.28	0.29	1.00	0.43	0.46
	-5	-5	-3	-4	-5	-6	6	-4	0	-1	-1
SIS	0.50	0.44	0.48	0.57	0.55	0.41	0.64	0.19	0.43	1.00	0.62
	-3	-4	-3	-3	-3	-2	-3	-4	1	0	0
ALT	0.72	0.59	0.67	0.61	0.73	0.56	0.71	0.24	0.46	0.62	1.00
	-3	-4	-3	-3	-3	-3	-3	-3	1	0	0

**Note:** \* For an ordered pair of stations, the first one is given in the first column of the table, while the second one in the first row. The optimal time shift is indicated under the estimate of correlation coefficient. Clusters corresponding to the stations of Southern Hemisphere and Northern Hemisphere are colored with yellow and blue, respectively

However, Table 3 data show that in the majority of cases the processes of atmospheric transmission cannot ensure substantial similarity of long-term series of seasonal deviations of concentrations of N<sub>2</sub>O and, consequently, of the other two gases. As a matter of fact, N<sub>2</sub>O has practically no sinks in the troposphere, and its lifetime in the atmosphere exceeds 100 years (Myhre et al., 2013). Therefore, N<sub>2</sub>O seasonal variations at the stations can be driven by two processes only: global emissions and atmospheric transmission. The first process is individual for each of the gases, while the second one is common. In general, the latter process, as inferred from the N<sub>2</sub>O data, does not ensure the discernible similarity of the time series of deviations at different stations.

The situation with CO<sub>2</sub> and CH<sub>4</sub> is different. As calculations show, (B-A)-series have high correlations even for the stations that are highly distanced from each other. The deviations have seasonal cyclicity and a rather stable form.

(B-A)-series for CO<sub>2</sub> of stations ALT and MLO are displayed in Fig. 7a, and Fig. 7b shows the ALT and SPO series. Correlation coefficients for these series are estimated, respectively, at 0.95 (MLO series is shifted backward in time for 1 month) and 0.87 (SPO series is shifted forward in time for 5 months). Correlations are high, although the stations are very far from each other: ALT is at the high latitudes of the Arctic, MLO is in the tropical part of the Pacific Ocean, SPO is at the South Pole.

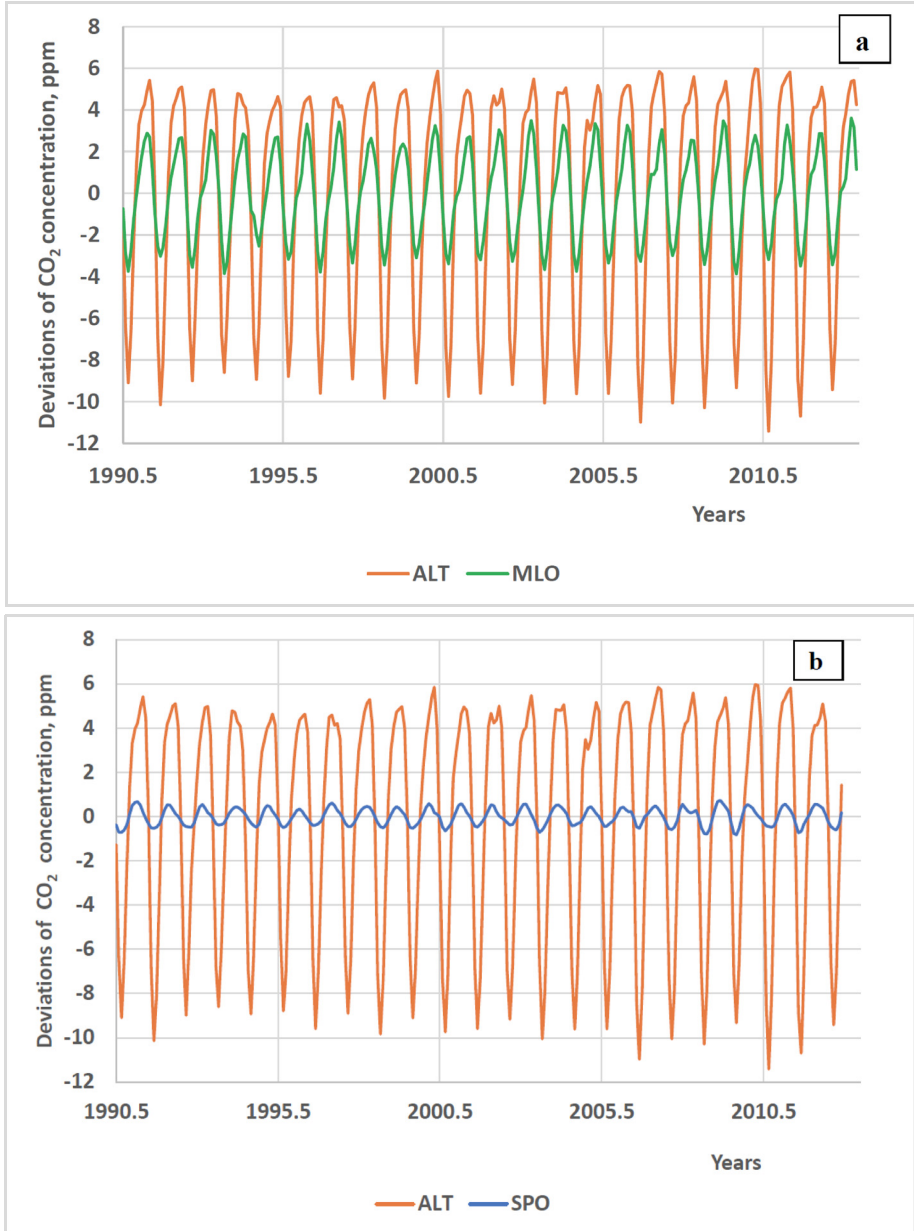


**Figure 7.** Seasonal deviations of CO<sub>2</sub> concentration: a) at stations ALT and MLO (MLO series is shifted backward in time for 1 month); b) at stations ALT and SPO (SPO series is shifted forward in time for 5 months)

It is typical for the whole set of stations that amplitude of deviations of the series decreases in southward direction.

Correlation coefficients for  $(B-A)$ -series of  $\text{CO}_2$  are given in Table 4. For the extratropical stations of both hemispheres, the correlation is high (from 0.8 to 0.9 and more) under respective optimal time shifts. The coefficients are especially high (more than 0.9) for the Northern Hemisphere stations. They are much lower for tropical stations CRI and CFA: from 0.5 to 0.8.

**Table 4.** Estimates of correlations for the time series of seasonal deviations of  $\text{CO}_2$  concentration\*

	SPO	MAA	CYA	MQA	CGO	CFA	CRI	MLO	ESP	SIS	ALT
SPO	1.00	0.91	0.91	0.86	0.91	0.51	0.71	0.87	0.86	0.88	0.87
	0	0	0	-1	0	2	5	-6	5	5	5
MAA	0.91	1.00	0.91	0.87	0.93	0.49	0.77	0.90	0.87	0.90	0.84
	0	0	0	-1	0	2	5	-5	5	5	-6
CYA	0.91	0.91	1.00	0.91	0.93	0.48	0.75	0.89	0.84	0.85	0.83
	0	0	0	0	0	2	5	-5	5	5	-6
MQA	0.86	0.87	0.91	1.00	0.88	0.53	0.72	0.86	0.81	0.85	0.84
	1	1	0	0	0	2	-6	-5	6	6	6
CGO	0.91	0.93	0.93	0.88	1.00	0.53	0.74	0.87	0.81	0.84	0.80
	0	0	0	0	0	2	5	-5	5	5	-6
CFA	0.51	0.49	0.48	0.53	0.53	1.00	0.48	0.53	0.51	0.51	0.50
	-2	-2	-2	-2	-2	0	3	5	4	4	4
CRI	0.71	0.77	0.75	0.72	0.74	0.48	1.00	0.77	0.60	0.64	0.69
	-5	-5	-5	6	-5	-3	0	2	0	0	1
MLO	0.87	0.90	0.89	0.86	0.87	0.53	0.77	1.00	0.93	0.94	0.95
	6	5	5	5	5	-5	-2	0	-1	-1	-1
ESP	0.86	0.87	0.84	0.81	0.81	0.51	0.60	0.93	1.00	0.98	0.98
	-5	-5	-5	-6	-5	-4	0	1	0	0	0
SIS	0.88	0.90	0.85	0.85	0.84	0.51	0.64	0.94	0.98	1.00	0.98
	-5	-5	-5	-6	-5	-4	0	1	0	0	0
ALT	0.87	0.84	0.83	0.84	0.80	0.50	0.69	0.95	0.98	0.98	1.00
	-5	6	6	-6	6	-4	-1	1	0	0	0

**Note:\*** For an ordered pair of stations, the first one is given in the first column of the table, while the second one in the first row. The optimal time shift is indicated under the estimate of correlation coefficient. Clusters corresponding to the stations of Southern Hemisphere and Northern Hemisphere are colored with yellow and blue, respectively.

As clear from Table 4, the optimal shifts reflect latitudinal seasonality. For the stations of the middle and high latitudes, the optimal time shifts of the Northern Hemisphere stations against Southern Hemisphere stations are from 5 to 7 months<sup>6</sup>.

<sup>6</sup>) Shifts for (-5) or (-6) months are the seasonal equivalent of shifts for 7 and 6 months, respectively.

Seasonality of oscillations of carbon dioxide concentration was described in the classical work (Keeling et al., 2005). It was explained by the intensification of photosynthesis in the warm season. Recently, seasonal oscillations have also been explored with remote sensing methods using satellite data, see for example (Rokotyan et al., 2014); numerous references on the topic are given in this publication.

Time series of seasonal deviations of CH<sub>4</sub> concentration at different CSIRO stations are even more similar that was demonstrated in detail in (Semenov, 2018). The estimates of correlation coefficients for the extratropical stations of the Southern Hemisphere exceeds 0.99, and only for the tropical station CFA they are from 0.94 to 0.96. These levels of correlations are reached under respective optimal time shifts

Under respective time shifts, (*B-A*)-series of the Northern Hemisphere stations also have high correlations, 0.7 to 0.8 in the majority of cases. However, they are noticeably smaller than those of the Southern Hemisphere.

Methane (*B-A*)-series of stations from different hemispheres are also quite similar, i.e., reveal high correlations, if the optimal time shifts are applied. For example, (*B-A*)-series of stations of the Southern Hemisphere have high correlations with high-latitude Arctic station Alert (ALT, 82.5°N). The coefficients of correlation between the series of those stations and the Alert series are as follows: 0.92 for SPO, 0.91 for MAA, 0.91 for CYA, 0.94 for MQA, and 0.89 for CFA. However, a 5-month backward time shift should be applied to the ALT series to reach such levels of correlation.

In conclusion of this section, Figure 8 presents the correlation coefficients of (*B-A*)-series for CH<sub>4</sub> and CO<sub>2</sub> obtained under optimal time shifts of CO<sub>2</sub> series. Such values are reached at the extratropical stations with no time shift of with a one-month backward time shift.

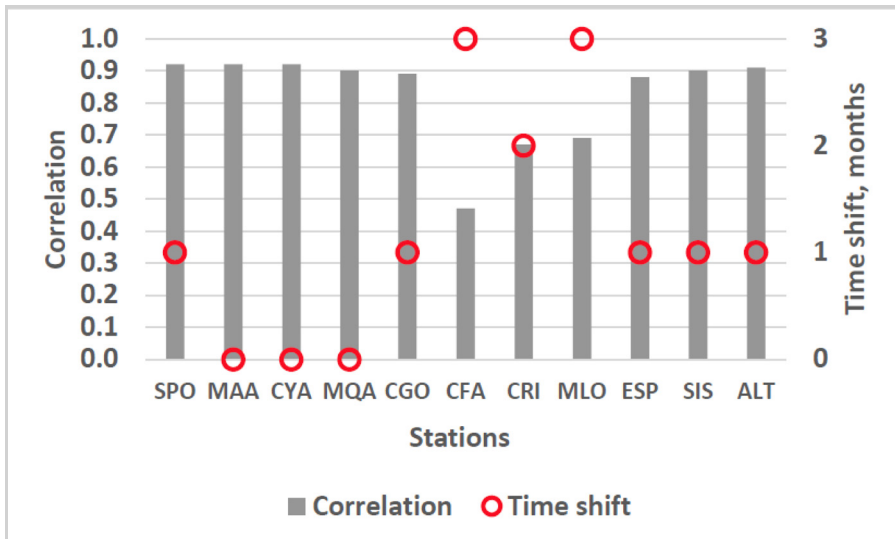


**Figure 8.** Estimates of correlation coefficients for the series of seasonal deviations of CH<sub>4</sub> and CO<sub>2</sub> concentrations (the left vertical axis) obtained under optimal time shifts of CO<sub>2</sub> series (the right vertical axis)

Correlations at the extra-tropical stations are noticeably high, more than 0.88 and exceed 0.9 in the majority of cases. This supports a hypothesis that the seasonal deviations of CO<sub>2</sub> and CH<sub>4</sub> concentrations are caused basically by common factor which has very strict seasonal manifestation. Logically, the seasonal variability of the solar radiation flux reaching the Earth's surface could serve as such factor. Its increase both stimulates photosynthesis of terrestrial and oceanic plants (causes CO<sub>2</sub> removal from the atmosphere) and the enrichment of the atmosphere with hydroxyl (increases atmospheric CH<sub>4</sub> depletion).

All optimal shifts obtained are backward. This means that 'CH<sub>4</sub> events' occur in advance of 'CO<sub>2</sub> events'. In particular, the period of decrease in methane concentration begins earlier than for carbon dioxide.

### Conclusions

The results of the above empirical analysis of variations of CO<sub>2</sub>, CH<sub>4</sub> and N<sub>2</sub>O concentrations at CSIRO global monitoring stations can be summarized as follows.

For each of three gases, the long-term trends of concentrations in the surface layer of the atmosphere are similar at all stations on the yearly time scale, i.e., for 12-months running averages (*A*-series). Series for CO<sub>2</sub> and CH<sub>4</sub> of the station Cape Rama is an exception; probably the station is under the influence of substantial local or regional emission sources.

Time series of differences of bimestrial running averages and 12-month running averages of monthly means (*B-A*-series) characterize seasonal variability of gases' concentrations. For CO<sub>2</sub> and CH<sub>4</sub>, these deviations have pronounced seasonality and rather stable form of intra-annual oscillations. For CO<sub>2</sub> and CH<sub>4</sub>, the correlation coefficients of these time series of extratropical stations under optimal time shifts occurred high, even for stations of different hemispheres. The optimal shifts are of the seasonal type.

These features are not typical of N<sub>2</sub>O. Therefore, such similarity cannot be ensured by the atmospheric transmission process being common for all three gases.

Similarity of series of seasonal variations of CO<sub>2</sub> and CH<sub>4</sub> concentrations at different stations support the following concept: the variations are driven by, respectively, the process of CO<sub>2</sub> removal from the atmosphere due to plants' photosynthesis and methane depletion in reactions with hydroxyl; seasonal changes in these processes are associated with seasonal oscillations of the solar radiation flux reaching the Earth's surface.

### Acknowledgments

The authors are thankful to Paul Krummel and Ray Langenfelds (CSIRO) for useful consultations on the monitoring data.

### References

Rokotyán N.V., Imasu R., Zakharov V.I., Gribanov K.G., Khamaturova M.Yu. 2014. The amplitude of the CO<sub>2</sub> seasonal cycle in the atmosphere of Ural by ground-based and satellite remote sensing techniques. – *Optika Atmosfery I Okeana*, vol. 27, No. 9, pp. 819-825 [in Russian].

Forster P., Ramaswamy V., Artaxo P., Bernsten T., Betts R., Fahey D.W., Haywood J., Lean J., Lowe D.C., Myhre G., Nganga J., Prinn R., Raga G., Schulz M., Van Dorland R. 2007. Changes in Atmospheric Constituents and in Radiative Forcing. – In: *Climate Change 2007: The Physical Science Basis. Contribution of Working Group I to the Fourth Assessment Report of the Intergovernmental Panel on Climate Change* /Solomon, S., D. Qin, M. Manning, Z. Chen, M. Marquis, K.B. Averyt, M.Tignor and H.L. Miller (eds.). – Cambridge University Press, Cambridge, United Kingdom and New York, NY, USA.

Keeling C.D., Piper S.C., Bacatow R.B., Wahlen M., Whorf T.P., Heimann P.M., Meijer H.A. 2005. Atmospheric CO<sub>2</sub> and <sup>13</sup>CO<sub>2</sub> exchange with the terrestrial biosphere and oceans from 1978 to 2000: observations and carbon cycle implications. – In "A History of Atmospheric CO<sub>2</sub> and its effects on Plants, Animals, and Ecosystems" /editors, Ehleringer, J.R., T. E. Cerling, M. D. Dearing. – Springer Verlag, New York, pp. 83-113.

Myhre G., Shindell D., Bréon F.-M., Collins W., Fuglestedt J., Huang J., Koch D., Lamarque J.-F., Lee D., Mendoza B., Nakajima T., RobockA., Step-hens G., Takemura T., Zhang H. 2013. Anthropogenic and Natural Radiative Forcing. – In: *Climate Change 2013: The Physical Science Basis. Contribution of Working Group I to the Fifth Assessment Report of the Intergovernmental Panel on Climate Change* /Stocker, T.F., D. Qin, G.-K. Plattner, M. Tignor, S.K. Allen, J. Boschung, A. Nauels, Y. Xia, V. Bex and P.M. Midgley (eds.). – Cambridge University Press, Cambridge, United Kingdom and New York, NY, USA.

Semenov S.M. 2018. Similarity of present-day variations in methane background concentrations in the surface layer of the atmosphere at different latitudes. – *Fundamental and Applied Climatology*, No. 3, pp. 124-137. Doi: 10.21513/2410-8758-2018-3-124-137.

Steele L.P., Krummel P.B., Langenfelds R.L. 2007. Atmospheric CO<sub>2</sub> concentrations from sites in the CSIRO Atmospheric Research GASLAB air sampling network (August 2007 version). – In *Trends: A Compendium of Data on Global Change*. – Carbon Dioxide Information Analysis Center, Oak Ridge National Laboratory, U.S. Department of Energy, Oak Ridge, TN, U.S.A.

Voulgarakis A., Naik V., Lamarque J.F., Shindell D.T., Young P., Prather M.J., Wild O., Field R., Sudo K., Szopa S., Zeng G. 2013. Analysis of present day and future OH and methane lifetime in the ACCMIP simulations. – *Atmospheric Chemistry and Physics*, vol. 13, pp. 2563-2587. Doi: 10.5194/acp-13-2563-2013.

*Submitted: 01.11.2018*

*Revised:03.12.2018*

Referencing this paper:

Semenov S.M., Ran'kova E. Ya. 2018. The features of multiyear changes and seasonal variability of present-day background concentrations of CO<sub>2</sub>, CH<sub>4</sub>, and N<sub>2</sub>O at the global monitoring stations. *Fundamental and Applied Climatology*, vol. 4, pp. 105-121. DOI: 10.21513/2410-8758-2018-4-105-121.

Translation from Russian. The original is published in this volume, pp. 71-87.

---